

Cation-Dependent Stability of Subtilisin[†]

Patrick A. Alexander, Biao Ruan, and Philip N. Bryan*

Center for Advanced Research in Biotechnology, University of Maryland Biotechnology Institute,
9600 Gudelsky Drive, Rockville, Maryland 20850

Received April 19, 2001; Revised Manuscript Received July 2, 2001

ABSTRACT: Subtilisin BPN' contains two cation binding sites. One specifically binds calcium (site A), and the other can bind both divalent and monovalent metals (site B). By binding at specific sites in the tertiary structure of subtilisin, cations contribute their binding energy to the stability of the native state and increase the activation energy of unfolding. Deconvoluting the influence of binding sites A and B on the inactivation rate of subtilisin is complicated, however. This paper examines the stabilizing effects of cation binding at site B by using a mutant of subtilisin BPN' which lacks calcium site A. Using this mutant, we show that calcium binding at site B has relatively little effect on stability in the presence of moderate concentrations of monovalent cations. At [NaCl] = 100 mM, site B is $\geq 98\%$ occupied with sodium, and therefore its net occupancy with a cation varies little as subtilisin is titrated with calcium. Exchanging sodium for calcium results in a 5-fold decrease in the rate of inactivation. In contrast, because of the high selectivity of site A for calcium, its occupancy changes dramatically as calcium concentration is varied, and consequently the inactivation rate of subtilisin decreases ~ 200 -fold as site A becomes saturated with calcium, irrespective of the concentration of monovalent cations.

Cations have been shown to play an important role in stabilizing proteins by binding at specific sites in their tertiary structure. Examples where metal binding makes a pronounced contribution to the stability of proteins are numerous (1–9). Extracellular microbial proteases are examples of very robust proteins which typically contain one or more cation binding sites. For example, thermolysin, from the thermophilic organism *Bacillus thermoproteolyticus*, contains four Ca^{2+} binding sites (10). The contribution of Ca^{2+} binding sites to the ΔG of unfolding for thermolysin was reported to be between 8.1 and 9.2 kcal/mol (11). The thermophilic fungal proteases proteinase K and thermitase have two and three calcium binding sites, respectively, which make large contributions to their high stability (12–14).

Subtilisin BPN' is a 275 amino acid serine protease secreted from the soil bacterium *Bacillus amyloliquefaciens*. High-resolution X-ray structures of subtilisin BPN', as well as numerous homologues (14–17), have revealed details of a conserved, high-affinity, calcium binding site, termed site A. A second site (site B) is less conserved and has weaker affinity for calcium (Figure 1).

Calcium at site A is coordinated by five carbonyl oxygen ligands and one aspartic acid. Four of the carbonyl oxygen ligands to the calcium are provided by a loop comprising amino acids 75–83. The geometry of the ligands is that of a pentagonal-bipyramid whose axis runs through the carbonyls of 75 and 79. The other ligands in the loop are the delta oxygen of N77 and the carbonyl oxygen of V81. On one side of the loop is the bidentate carboxylate (D41), while on the other side is the N-terminus of the protein and the side chain of Q2. The seven coordination distances range

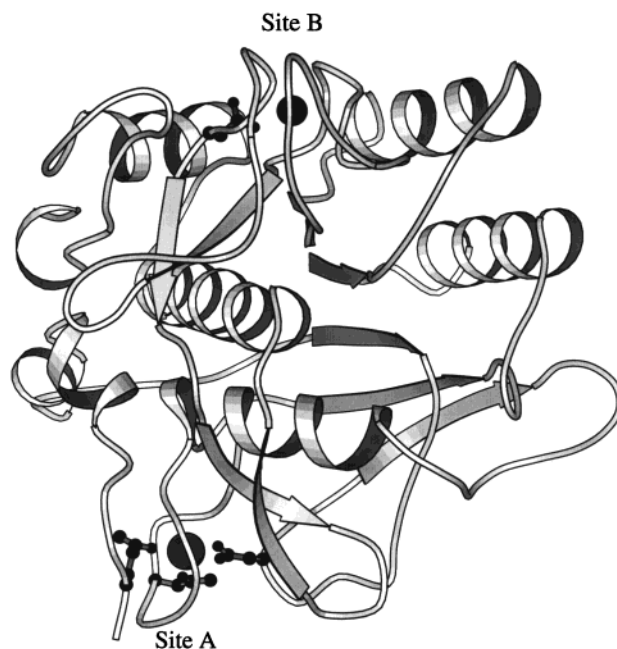


FIGURE 1: Ribbon drawing depicting the α -carbon backbone of subtilisin. Cation binding sites A and B are depicted with only side chain ligands shown.

from 2.3 to 2.6 Å, the shortest being to the aspartyl carboxylate. Three hydrogen bonds link the N-terminal segment to loop residues 78–82 in a parallel-beta arrangement.

The binding parameters of calcium at site A have been determined previously by titration calorimetry: $\Delta H_{\text{binding}} = -11$ kcal/mol and $\Delta G_{\text{binding}} = -9.3$ kcal/mol at 25 °C (18). Thus, the binding of calcium is primarily enthalpically driven with only a small net loss in entropy [$\Delta S_{\text{binding}} = -6.7$ cal/(°C·mol)]. This is surprising since transfer of calcium into

[†] Supported by NIH Grant GM42560.

* To whom correspondence should be addressed. Tel: 301-738-6220. FAX: 301-738-6255. E-mail: bryan@umbi.umd.edu.

water results in a loss of entropy of $-60 \text{ cal}/(^{\circ}\text{C}\cdot\text{mol})$. Therefore, the freeing of water upon calcium binding to the protein will make a major contribution to the overall ΔS of the process. The gain in solvent entropy upon binding must be compensated for by a loss in entropy of the protein. Presumably, the loop amino acids 75–83 and the first few N-terminal residues have increased mobility when calcium is absent from the A site.

A second ion binding site (site B) is located 32 Å from site A in a shallow crevice between two segments of the polypeptide chain near the surface of the molecule (Figure 1). Evidence that site B binds calcium comes from determining the occupancy of the site in a series of X-ray structures from crystals grown in 50 mM NaCl with calcium concentrations ranging from 1 to 40 mM (19). In the absence of excess calcium, this locus was found to bind a sodium ion. The binding of these two ions appears to be mutually exclusive so that as the calcium concentration increases, the sodium ion is displaced, and a water molecule appears in its place directly coordinated to the bound calcium (19). When calcium is bound, the coordination geometry of this site closely resembles a distorted pentagonal-bipyramid. Three of the ligands are derived from the protein and include the carbonyl oxygen atom of E195 and the two side-chain carboxylate oxygens of D197. Four water molecules complete the coordination sphere. When sodium is bound, its position is removed by 2.7 Å from that of calcium, and the ligation pattern changes. The sodium ligands derived from the protein include a side-chain carboxylate oxygen of D197 and the carbonyl oxygen atoms of G169, Y171, V174, and E195. Two water molecules complete the coordination sphere.

By binding at specific sites in the tertiary structure of subtilisin, cations contribute their binding energy to the stability of the native state and increase the activation energy of unfolding. The rate of thermal inactivation of subtilisin is decreased about 1000-fold as the calcium concentration is increased from near zero (excess EDTA)¹ to 100 mM CaCl_2 (19). Deconvoluting the influence of binding sites A and B on the inactivation rate is complicated, however. This paper examines the stabilizing effects of cation binding at site B by using a mutant of subtilisin BPN' which lacks calcium site A. Following the characterization of site B, we are able to assess the relative contributions of each site on stability.

MATERIALS AND METHODS

Cloning and Expression. The subtilisin gene from *Bacillus amyloliquefaciens* (subtilisin BPN') has been cloned, sequenced, and expressed at high levels from its natural promoter sequences in *Bacillus subtilis* (20, 21). All mutant genes were recloned into a pUB110-based expression plasmid and used to transform *B. subtilis*. The *B. subtilis* strain used as the host contains a chromosomal deletion of its subtilisin gene and therefore produces no background wild-type (wt) activity (22). Mutagenesis of the cloned prodomain gene was performed according to the oligonucleotide-directed

in vitro mutagenesis system, version 2 (Amersham International plc). Single-strand plasmid DNA was sequenced according to Sequenase (United States Biochemical).

Protein Purification. Subtilisin BPN' and a variant lacking site A, S152, were expressed in a 1.5 L New Brunswick fermentor at a level of $\sim 200 \text{ mg/L}$. After fermentation, 16 g of Tris-base and 22 g of CaCl_2 (dihydrate) were added to $\sim 1400 \text{ mL}$ of broth. Cells and precipitate were pelleted in 250 mL bottles by centrifugation at 12000g for 30 min, 4 $^{\circ}\text{C}$. Acetone (70% final volume) was added to the supernatant. The 70% acetone mixture was then centrifuged in 500 mL bottles at 12000g for 30 min, 4 $^{\circ}\text{C}$. The pellet was resuspended in $\sim 150 \text{ mL}$ of 20 mM HEPES, pH 7.0, 1 mM CaCl_2 . Resuspended material was centrifuged at 12000g for 10 min, 4 $^{\circ}\text{C}$, to remove insoluble material. Using a vacuum funnel, the sample was passed over 150 g of DE52, equilibrated in 20 mM HEPES, pH 7.0. The DE52 was washed 2 times with 150 mL of 20 mM HEPES, 1 mM CaCl_2 buffer, and all the washes were pooled. Solid $(\text{NH}_4)_2\text{SO}_4$ was added to the sample to a final concentration of 1.8 M. Final purification was carried out using a $2 \times 30 \text{ cm}$ Poros HP 20 column on a Biocad Sprint. The sample was loaded and washed in 1.8 M $(\text{NH}_4)_2\text{SO}_4$, 20 mM HEPES, pH 7.0, and then eluted with a linear gradient [1.8–0 M $(\text{NH}_4)_2\text{SO}_4$ in 20 mM HEPES, pH 7.0]. Subtilisin BPN' eluted at a conductivity of 108 mS and S152 at 96 mS.

Activity Assays. Assays of peptidase activity were performed by monitoring the hydrolysis of sAAPF-pNA as described by (23). The [subtilisin] was determined using 1 mg/mL = 1.17 at 280 nm. For S152 which has one fewer tyrosine, the 1 mg/mL at 280 nm was calculated to be 1.12 (or $0.96 \times \text{wt}$), based on the loss of one Tyr residue (24).

Differential Scanning Calorimetry (DSC). DSC measurements were performed on the inactive subtilisin mutant, S221C,² using a Hart 7707 DSC heat conduction scanning microcalorimeter interfaced with an IBM personal computer (18). The temperature was increased from 20 to 110 $^{\circ}\text{C}$ at a scan rate of 30 or 60 $^{\circ}\text{C/h}$. The volume of all protein and control solutions was near 0.70 mL per ampule. The concentration of S221C subtilisin was 3 mg/mL. Each experiment was comprised of four segments: (1) the first upward scan from 20 to 110 $^{\circ}\text{C}$; (2) the first downward scan from 110 to 20 $^{\circ}\text{C}$; (3) a second upward scan from 20 to 110 $^{\circ}\text{C}$; and (4) a second downward scan returning to 20 $^{\circ}\text{C}$. The power input from an upward scan of buffer vs buffer was subtracted from the first upward scan to obtain the excess power input for the unfolding transitions. The excess power thermal scans were converted to excess heat capacity vs T scans by dividing by the scan rate.

Determination of Inactivation Rates. The kinetics of inactivation were determined as follows. Subtilisin at 1 μM concentration was dispensed in aliquots of 0.5 mL into 1 mL glass test tubes and covered with Parafilm. The tubes were placed in a circulating water bath at the appropriate temperature. At each time point, a tube was removed and quickly transferred to an ice bath. A 10 μL aliquot was removed, and residual activity was assayed in 990 μL of 1

¹ Abbreviations: DSC, differential scanning calorimetry; EDTA, disodium salt of ethylenediaminetetraacetic acid; sAAPF-pNA, succinyl-L-Ala-L-Ala-L-Pro-L-Phe-*p*-nitroanilide; Tris, tris(hydroxymethyl)aminomethane; $t_{1/2}$, half-life for a kinetic experiment; wt, wild type.

² A shorthand for denoting amino acid substitutions employs the single-letter amino acid code as follows: N218S denotes the change of asparagine 218 to serine.

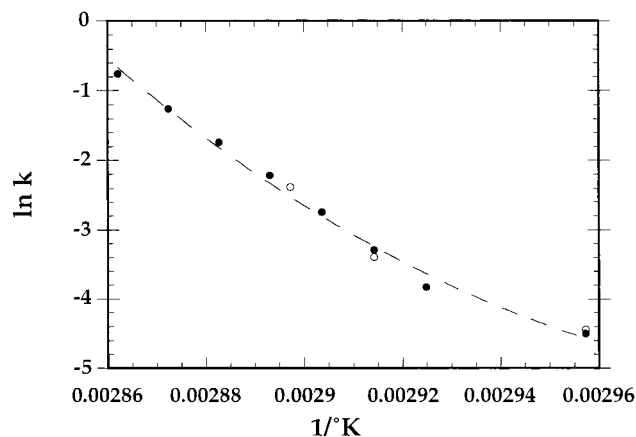


FIGURE 2: Comparison of the rates of irreversible thermal inactivation of S221C subtilisin with the rate of thermal unfolding of wt subtilisin in 50 mM Tris-HCl, pH 8.0, 50 mM NaCl, 10 mM CaCl_2 , over the temperature range of 65–75 °C. Unfolding rates are measured by differential scanning calorimetry. Data are plotted as the natural logarithm of the rate constants vs $1/K$. Solid circles show the rate of unfolding, and open circles show the rate of inactivation. The activation energy of both processes is ~ 80 kcal/mol at 65 °C.

mM sAAPF-pNA, 0.1 M Tris-HCl, pH 8.0, 0.1 M NaCl. The inactivation time course was followed over four half-lives.

RESULTS

Kinetics of Inactivation and the Unfolding Rate. Under the conditions which we have employed in this paper ($[\text{subtilisin}] \leq 1 \mu\text{M}$ and temperature ≥ 65 °C), the rate of thermal inactivation of subtilisin is characterized by a single-exponential decay curve whose time constant is determined by the rate of subtilisin unfolding. This can be demonstrated by comparing the rate of unfolding of an inactive (S221C) variant of subtilisin by scanning calorimetry with the rate of thermal inactivation of the corresponding active version (Figure 2). The proteolytic activity of the C221C mutant is about 50 000 times less than wt subtilisin, so that the rate of unfolding can be observed independent of autoproteolysis (25–27). A rate constant for unfolding of the S221C mutant was calculated from the DSC trace using the equation: $k = \nu C_p / (Q_t - Q)$, where ν is the scan rate, C_p is the excess heat capacity, Q_t is the total heat of the unfolding process, and Q is the heat evolved at a given temperature (28).

Kinetics of Irreversible Inactivation of Subtilisin vs [Calcium]. The calcium dependence of the inactivation rate of wild-type subtilisin BPN' is shown in Figure 3. The calcium concentration was varied from 100 μM to 100 mM. The invariant buffer components were 100 mM Tris-HCl, pH 8.0, 100 mM NaCl. The rate of inactivation at 65 °C decreases by ~ 100 -fold as [calcium] is increased from 100 μM to 100 mM. Understanding the physical basis for this calcium effect requires examination of the mechanism of thermal inactivation and the affinities of the two ion binding sites. To separate the influence of site B on cation-dependent stability from that of site A, we chose to analyze a mutant of subtilisin which lacks site A.

Construction of a Subtilisin Mutant Lacking Site A (Subtilisin S152). The calcium binding loop of site A is formed from a nine amino acid bubble in the last turn of an α -helix, comprising amino acids 63–85 (helix C) (17). In

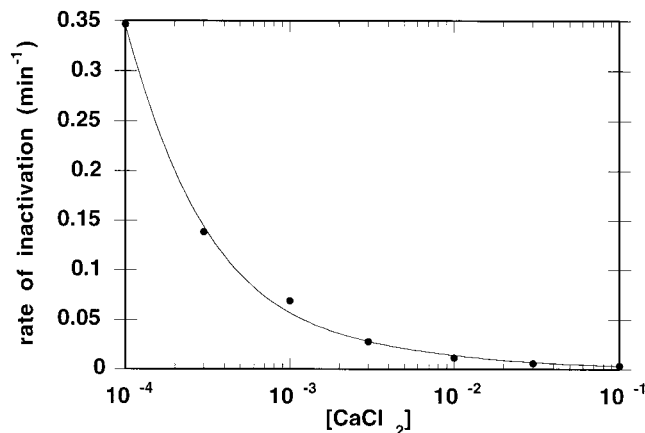


FIGURE 3: Rates of thermal inactivation of subtilisin BPN' at 65 °C are plotted as a function of calcium concentration. The data are fit to mechanism 3 in the text.

previous work, we have shown that deleting amino acids 75–83 creates an uninterrupted helix and abolishes the calcium binding potential at site A (18, 29, 30). X-ray structures have shown that except for the region of the deleted calcium binding loop, the structures of the mutant and wild-type protein are remarkably similar considering the size of the deletion. The structures of subtilisin with and without the deletion superimpose with an rms difference between 261 C α positions of 0.17 Å. Following deletion of amino acids 75–83, α -helix C is uninterrupted and shows normal helical geometry over its entire length (29). Nevertheless regions of subtilisin which were adjacent to the 75–83 loop have lost many favorable interactions. The N-terminus of the wild-type protein lies beside the site A loop, furnishing one calcium coordination ligand, the side chain oxygen of Q2. The deletion leaves residues 1–4 disordered. In addition to the N-terminal amino acids, the regions of the mutant most affected by deletion are the 36–44 ω -loop, the 63–85 α -helix, and the 202–219 β -strand. Consequently, a number of compensating mutations were identified and introduced into the deletion mutant to restore high stability. This work is described in detail in Strausberg et al. (31) and in the accompanying paper (33). The mutant used here to characterize site B is denoted S152 and contains the following mutations: Q2K, S3C, P5S, K43N, A73L, $\Delta 75$ –83, E156S, G166S, G169A, S188P, Q206C, N212G, K217L, N218S, T254A, and Q271E.

Inactivation of S152 Subtilisin vs [Sodium] and [Calcium]. Rates of inactivation as a function of [calcium] were determined for S152 as for wild-type subtilisin (0.1M Tris-HCl, pH 8.0, 100 mM NaCl), except that the inactivation temperature was 70 °C because of the higher stability of S152. The rate of inactivation of S152 decreases by ~ 5 -fold as [calcium] is increased from 100 μM to 100 mM. Thus, calcium binding at site B has relatively little influence on S152 stability in the presence of 100 mM NaCl. In contrast, the inactivation rate of wild-type subtilisin decreased ~ 100 -fold as [calcium] was increased from 100 μM to 100 mM.

We next evaluated the influence of [NaCl] on the inactivation rate of S152. The [NaCl] was varied from 100 μM to 100 mM in 0.1 M Tris-HCl, pH 8.0. Tris is a large, soft cation which has little influence on the stability of subtilisin (data not shown). The results are summarized in Figure 4A.

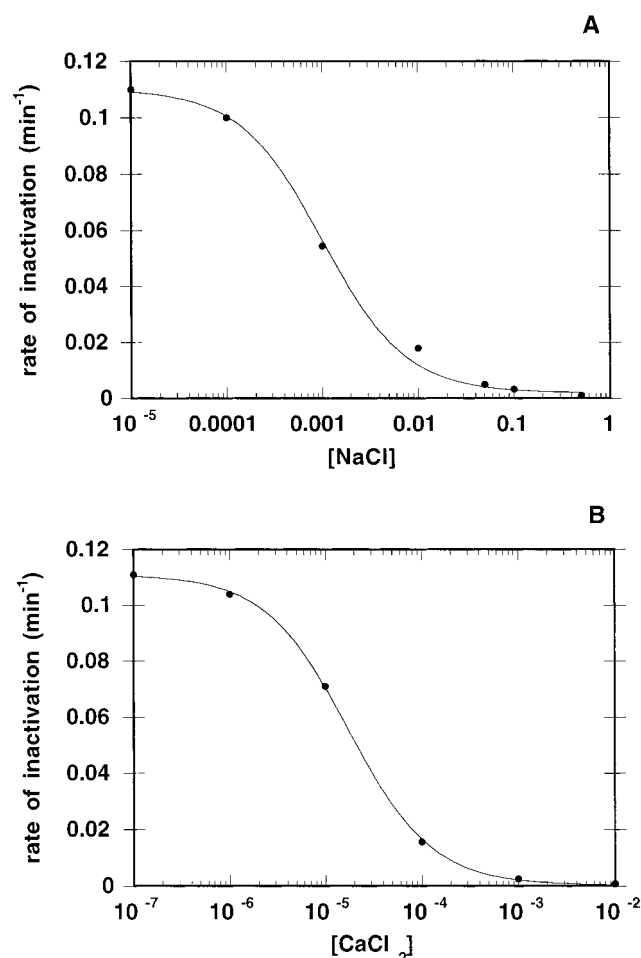
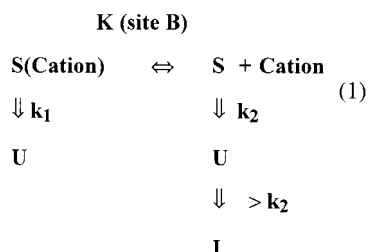


FIGURE 4: (A) Rates of thermal inactivation of subtilisin S152 at 70 °C are plotted as a function of [sodium]. The data are fit to mechanism 1 in the text with $K(\text{site B}) = 1 \text{ mM}^{-1}$. (B) Rates of thermal inactivation of subtilisin S152 at 70 °C are plotted as a function of [calcium]. The data are fit to mechanism 1 in the text with $K(\text{site B}) = 60 \text{ mM}^{-1}$.

The rate of inactivation of S152 at 75 °C decreased by 160-fold as [NaCl] was increased from 100 μM to 100 mM. These data were used to determine the binding affinity of sodium to site B. In the presence of excess cation, the inactivation rate of S152 subtilisin can be diagrammed as follows:



S denotes native subtilisin, U denotes unfolded subtilisin, and I denotes irreversibly inactivated subtilisin. In excess cation (e.g., $\geq 100 \mu\text{M}$) and at temperatures at which unfolding of the free protein is slower than cation binding (rapid binding equilibrium model), the rate of inactivation will be determined by the fraction of each native species times its unfolding rate. Fitting the inactivation data to mechanism 1 yields a binding constant of sodium for site B of 1 mM^{-1} .

Table 1: Affinity of Site B for Various Cations^a

cation	Ca	K	Na	NH ₄	Li
K_a	67 mM^{-1}	10 mM^{-1}	1.3 mM^{-1}	5 mM^{-1}	12 mM^{-1}
ionic radius	0.99 Å	1.33 Å	0.95 Å	1.52 Å	0.60 Å

^a Binding affinities were determined by measuring the inactivation rate of $\Delta 75\text{--}83$ subtilisin as a function of [cation].

The same experiment was repeated using CaCl_2 , instead of NaCl. The $[\text{CaCl}_2]$ was varied from 100 μM to 100 mM in 0.1 M Tris-HCl, pH 8.0. The results are summarized in Figure 4B. Fitting the inactivation data to mechanism 1 yields a binding constant of calcium for site B of 60 mM^{-1} , about 60-fold tighter than sodium.

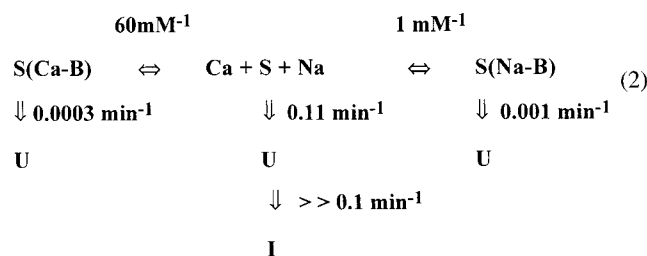
Since sodium and calcium compete for occupancy of site B, one can calculate the influence of one ligand on the binding of the other according to the equations:

$$[\text{SCa}]/[\text{S}_{\text{total}}] = K_{\text{S-Ca}}[\text{Ca}]/(1 + K_{\text{S-Ca}}[\text{Ca}] + K_{\text{S-Na}}[\text{Na}])$$

and

$$[\text{SNa}]/[\text{S}_{\text{total}}] = K_{\text{S-Na}}[\text{Na}]/(1 + K_{\text{S-Ca}}[\text{Ca}] + K_{\text{S-Na}}[\text{Na}])$$

where $[\text{SCa}]/[\text{S}_{\text{total}}]$ is the fraction of subtilisin bound to calcium, $[\text{SNa}]/[\text{S}_{\text{total}}]$ is the fraction of subtilisin bound to sodium, $K_{\text{S-Ca}}$ is the binding constant for calcium (60 mM^{-1}), and $K_{\text{S-Na}}$ is the binding constant for sodium (1 mM^{-1}). In the presence of 100 mM NaCl, the observed binding constant of site B for calcium is $\sim 0.6 \text{ mM}^{-1}$. The calcium dependence of inactivation of S152 in 0.1 M NaCl at 70 °C can be accounted for using the following model:



S(Ca-B) denotes native S152 with calcium in site B, and S(Na-B) denotes native S152 with sodium in site B.

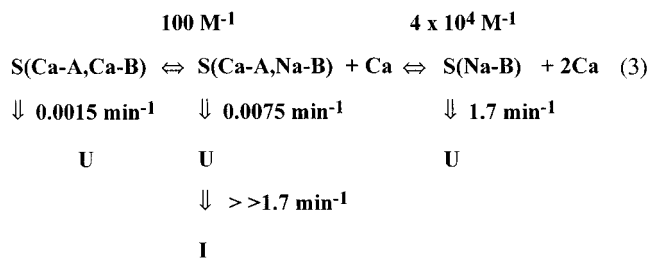
Rate of Thermal Inactivation of S152 as a Function of [Ca], [Na], [K], [NH₄], and [Li]. To determine the preferences of site B for other monovalent cations, we measured the rate of inactivation of S152 subtilisin as a function of [KCl], [NH₄Cl], and [LiCl]. By measuring inactivation rate for each cation and fitting the data to mechanism 1, the association constant to site B was determined for each (Table 1). The association of site B to ammonium, potassium, and lithium cations is greater than to sodium ($K_a = 12 \text{ mM}^{-1}$ for lithium, 10 mM^{-1} for potassium, 5 mM^{-1} for ammonium, and 1.0 mM^{-1} for sodium). The relative affinity of site B for different ions appears to be a function of both the net charge and the atomic radius of the cation. The ionic radii of calcium and sodium are similar (0.99 and 0.95 Å, respectively). Presumably the 2+ charge of calcium is responsible for its 60-fold higher affinity. The ionic radii of potassium and ammonium are similar (1.33 and 1.52 Å, respectively), and their binding affinities are similar. Lithium binds as tightly as potassium and ammonium, despite its

small ionic radius (0.60 Å). This may indicate that two lithium ions can be bound at site B.

DISCUSSION

The major finding of this paper is the determination of the ion affinities of site B in subtilisin. These findings have significant implications on the interpretation of the calcium-dependent stability of wild-type subtilisin. In the past, we (19) and others (32) have suggested that calcium binding to site B is responsible for the large decrease in the inactivation rate of subtilisin in the presence of millimolar concentrations of calcium. Reexamination of calcium-dependent stability data in light of a better understanding of the ion binding preferences of site B shows that the calcium binding at site B has relatively little effect on stability in the presence of moderate concentrations of monovalent cations. At [NaCl] = 0.1 M, site B is $\geq 98\%$ occupied with sodium, and therefore its net occupancy with a cation varies little as subtilisin is titrated with calcium. Exchanging sodium for calcium results in a 5-fold decrease in the rate of inactivation. The region of subtilisin around site B has a high charge density with two Glu, one Asp, one Arg, and one Lys within a 8 Å radius. Particularly striking is the close juxtaposition of Glu 251 and Asp 197. Cations therefore would be expected to stabilize the folded state. The specificity of site B for a particular cation is low, however.

The occupancy of the calcium-selective site A does change dramatically, as [calcium] is varied. Consequently, one can model the inactivation data for wild-type subtilisin from Figure 3 using a rapid binding equilibrium model:



S(Ca-A,Ca-B) denotes subtilisin with calcium in sites A and B, **S(Ca-A,Na-B)** denotes subtilisin with calcium in site A and sodium in site B, and **S(Na-B)** denotes subtilisin with no cation in site A and sodium in B. Figure 3 plots the rate of inactivation of BPN' at 65 °C as a function of calcium concentration. The data closely fit the mechanism when the K_a of site A for calcium is $4 \times 10^4 \text{ M}^{-1}$ (65 °C). Because the experiment is carried out in 0.1 M NaCl, site B of native subtilisin is occupied with either calcium or sodium, and the observed K_a of site B for calcium is 100 M^{-1} (65 °C). The rate of inactivation of subtilisin with both sites occupied with calcium is about 5 times slower than with site A occupied with calcium and site B with sodium, and about 1000 times slower than subtilisin with only site B occupied with sodium. Thus, in the presence of 0.1 M NaCl, calcium-dependent stabilization of subtilisin is dominated by site A rather than site B.

The structure of the calcium A site in subtilisin is fundamentally different from the more common EF hand calcium binding sites of calbindin, parvalbumin, calmodulin, α -lactalbumin, or troponin C. All of the protein ligands to

calcium in an EF hand structure are on a single loop of about 12 amino acids connecting 2 α -helices, and 3 or 4 of the side chain ligands to the calcium are aspartic acid or glutamic acid. By contrast, the protein ligands of the A site come from three noncontiguous regions of subtilisin, and only one of the ligands (D41) carries a formal charge. The K_a of the A site ($\sim 10^7 \text{ M}^{-1}$ at 25 °C) is comparable to those of EF hand structures, which range from 10^5 to 10^9 M^{-1} . Also, the binding of calcium to both types of site is enthalpically driven. A major difference in the A site, however, is that the on and off rates for calcium are 3–4 orders of magnitude slower. This difference may reflect that EF hand proteins are typically part of a calcium messenger system and are designed to be responsive to changes in calcium concentration in order to trigger various biological processes. In subtilisin, calcium is an integral part of the structure, and its association or dissociation probably requires significant but transient disruption in surrounding protein–protein interactions. This disruption in structure would explain the high activation energy and slow kinetics of calcium binding and dissociation. For example, breaking main-chain hydrogen bonds between the N-terminal region and the loop region would allow the relatively buried calcium a passageway into or out of the protein. On the basis of this, we have argued previously the calcium binding sites are common features of extracellular microbial proteases probably because of their large contribution to both thermodynamic and kinetic stability. The results presented here, however, show that stabilization of subtilisin by excess calcium at 65 °C is primarily a thermodynamic effect. That is, at [calcium] $\geq 100 \mu\text{M}$, the inactivation rates can be modeled by assuming that calcium binding to the native state remains at equilibrium. Only at [calcium] below $100 \mu\text{M}$ does the rate of calcium dissociation from site A begin to influence the inactivation rate noticeably.

A final implication of this work is that caution is required in interpreting mutations which alter the calcium-dependent stability of subtilisin. Most stabilizing mutations isolated to date affect the rate of subtilisin inactivation in a calcium-dependent manner. That is, most mutations stabilize only in the presence of excess calcium and not in the presence of calcium chelators, such as EDTA. As will be discussed in the following paper (33), the reason for this behavior is related to the indirect influence of the global stability of subtilisin on calcium binding at site A.

ACKNOWLEDGMENT

We thank Fenhong Song for oligonucleotide synthesis and Jaya Jagadeesh for help with DNA sequencing.

REFERENCES

- Filimonov, V. V., Pfeil, W., Tsalkova, T. N., and Privalov, P. L. (1978) *Biophys. Chem.* 8, 117–122.
- Stellwagon, E., and Wilgus, H. (1978) in *Biochemistry of Thermophily* (Friedman, S. M., Ed.) pp 228–232, Academic Press, New York.
- Chlebowski, J. F., Mabrey, S., and Falk, M. M. (1979) *J. Biol. Chem.* 254, 5745–5753.
- Mitani, M., Harushima, Y., Kuwajima, K., Ikeguchi, M., and Sugai, S. (1986) *J. Biol. Chem.* 261, 8824–8829.
- Stuart, D. I., Acharya, K. R., Walker, N. P. C., Smith, S. G., Lewis, M., and Phillips, D. C. (1986) *Nature* 324, 84–87.

6. Linse, S., Brodlin, P., Drakenberg, T., Thulin, E., Sellers, P., Elmdén, K., Grundström, T., and Forsén, S. (1987) *Biochemistry* 26, 6723–6735.
7. Roe, J. A., Butler, A., Scholler, D. M., Valentine, J. S., Marky, L., and Breslauer, K. L. (1988) *Biochemistry* 27, 950–958.
8. Bertazzon, A., Tian, G. H., Lamblin, A., and Tsong, T. Y. (1990) *Biochemistry* 29, 291–298.
9. Pace, C. N., and Grimesly, G. R. (1988) *Biochemistry* 27, 3242.
10. Matthews, B. W., Weaver, L. H., and Kester, W. R. (1974) *J. Biol. Chem.* 249, 8030–8044.
11. Voordouw, G., Milo, C., and Roche, R. S. (1976) *Biochemistry* 15, 3716–3724.
12. Meloun, B., Baudys, M., Kostka, V., Hausdorf, G., Frommel, C., and Hohne, W. E. (1985) *FEBS Lett.* 183, 195–200.
13. Betzel, C., Teplyakov, A. V., Harutyunyan, E. H., Sängler, W., and Wilson, K. S. (1990) *Protein Eng.* 3, 161–172.
14. Gros, P., Kalk, K. H., and Hol, W. G. J. (1991) *J. Biol. Chem.* 266, 2953–2961.
15. Bode, W., Papamokos, E., and Musil, D. (1987) *Eur. J. Biochem.* 166, 673–692.
16. Betzel, C., Kupsch, S., Papendorf, G., Hastrup, S., Branner, S., and Wilson, K. S. (1992) *J. Mol. Biol.* 223, 427–445.
17. McPhalen, C. A., and James, M. N. G. (1988) *Biochemistry* 27, 6582–6598.
18. Bryan, P., Alexander, P., Strausberg, S., Schwarz, F., Wang, L., Gilliland, G., and Gallagher, D. T. (1992) *Biochemistry* 31, 4937–4945.
19. Pantoliano, M. W., Whitlow, M., Wood, J. F., Rollence, M. L., Finzel, B. C., Gilliland, G., Poulos, T. L., and Bryan, P. N. (1988) *Biochemistry* 27, 8311–8317.
20. Wells, J. A., Ferrari, E., Henner, D. J., Estell, D. A., and Chen, E. Y. (1983) *Nucleic Acids Res.* 11, 7911–7925.
21. Vasantha, N., Thompson, L. D., Rhodes, C., Banner, C., Nagle, J., and Filpula, D. (1984) *J. Bacteriol.* 159, 811–819.
22. Fahnestock, S. R., and Fisher, K. E. (1987) *Appl. Environ. Microbiol.* 53, 379–384.
23. DelMar, E., Largman, C., Brodrick, J., and Geokas, M. (1979) *Anal. Biochem.* 99, 316–320.
24. Pantoliano, M. W., Whitlow, M., Wood, J. F., Dodd, S. W., Hardman, K. D., Rollence, M. L., and Bryan, P. N. (1989) *Biochemistry* 28, 7205–7213.
25. Neet, K. E., and Koshland, D. E., Jr. (1966) *Proc. Natl. Acad. Sci. U.S.A.* 56, 1606–1611.
26. Polgar, L., and Bender, M. L. (1967) *Biochemistry* 6, 610–620.
27. Abrahmsen, L., Tom, J., Burnier, J., Butcher, K. A., Kosiakoff, A., and Wells, J. A. (1991) *Biochemistry* 30, 4151–4159.
28. Sanchez-Ruiz, J. M., Lopez-Lacombe, J. L., Cortijo, M., and Mateo, P. L. (1988) *Biochemistry* 27, 1648–1652.
29. Gallagher, T. D., Bryan, P., and Gilliland, G. (1993) *Proteins: Struct., Funct., Genet.* 16, 205–213.
30. Almog, O., Gallagher, T., Tordova, M., Hoskins, J., Bryan, P., and Gilliland, G. L. (1998) *Proteins: Struct., Funct., Genet.* 31, 21–32.
31. Gilliland, G., Barnett, B. L., and Bryan, P. (1995) *Bio/Technology* 13, 669–673.
32. Braxton, S. B., and Wells, J. A. (1992) *Biochemistry* 31, 7796–7801.
33. Alexander, P. A., Ruan, B., Strausberg, S. L., and Bryan, P. N. (2001) *Biochemistry* 40, 10640–10644.

BI010797M